

CARRIER LIFETIME STUDIES OF STRONGLY COMPENSATED P-TYPE CZOCHRALSKI SILICON

D. Macdonald¹, A. Cuevas¹, M. Di Sabatino² and L. J. Geerligs³

¹Department of Engineering, The Australian National University, Canberra, ACT 0200 Australia.

Tel: +61 2 6125 2973, fax: +61 2 6125 0506, E-mail: daniel.macdonald@anu.edu.au

²SINTEF Materials and Chemistry, A. Getz v. 2B, 7465 Trondheim, Norway. E-mail: Marisa.Di.Sabatino@sintef.no

³Energy Research Centre of the Netherlands (ECN), PO Box 1, NL-1755 ZG Petten, The Netherlands.
E-mail: geerligs@ecn.nl

ABSTRACT: Carrier lifetimes have been measured in compensated *p*-type single-crystal silicon wafers. Trace amounts of interstitial iron were found to provide a convenient method for measuring the total concentrations of acceptors and donors in this material, based on measuring the re-pairing rate of iron-acceptor pairs, coupled with resistivity measurements and a suitable mobility model. The results were found to be in good agreement with dopant concentrations measured independently by glow-discharge mass spectrometry. In addition, there appears to be a reduction in the bulk lifetime in compensated wafers when compared to non-compensated wafers of similar net doping. Possible mechanisms behind this reduction are discussed.

Keywords: silicon, doping, recombination, compensation.

1 INTRODUCTION

As sections of the silicon solar cell industry move towards new, low-cost, solar-grade silicon feedstocks over the next several years, there is likely to be an increase in the amount of relatively heavily compensated silicon used for ingot growth. The impact of using such compensated silicon for solar cells is currently not well understood. In addition to a likely reduction in carrier mobilities, which could affect solar cell currents, the recombination lifetime may also be reduced. This could arise, for example, due to additional boron resulting in an increase in the detrimental impact of the B-O defect in materials containing oxygen [1]. Other dopant-related complexes may also exist. It is also conceivable that the compensated dopants of the minority carrier type (for example phosphorus in *p*-type silicon) could act as mild recombination centres in their own right [2]. Their recombination activity would almost certainly be quite weak, but this could be countered by their high concentrations. These effects could cause a noticeable reduction of the carrier lifetime when comparing compensated wafers with non-compensated wafers of similar net doping levels.

On the other hand, compensation may offer some advantages. Firstly, it can provide an inexpensive means of avoiding very low resistivity material made from cheap silicon feedstocks. Compensation could also help to mitigate the impact of some other recombination centres [3,4], by reducing the equilibrium majority carrier concentration. Therefore the impact of compensation on carrier lifetime is an important issue.

In this paper, we firstly describe a simple method for measuring both the acceptor N_A and donor N_D concentrations in compensated silicon wafers (as opposed to the *net* dopant concentration $N_A - N_D$ or $N_D - N_A$ usually obtained via resistivity measurements), using iron-acceptor pairing kinetics. This information reveals the extent of compensation of a wafer, and is otherwise not easily obtained. Secondly, we examine the impact of compensation on the bulk lifetime, and observe a reduction by approximately a factor of two in Quasi-Steady-State Photoconductance (QSSPC) lifetime measurements for the compensation levels studied.

2 EXPERIMENTAL DETAILS

The samples used were cleaved sections of 155×155 mm pseudo-square, *p*-type, <100>-oriented Czochralski-grown silicon wafers. There were wafers from three control ingots (non-compensated), which were boron-doped, and had resistivities of approximately 4.4, 1.0 and 0.4 Ωcm , and also two compensated ingots, doped with both boron and phosphorus, with resistivities of approximately 1.6 and 0.47 Ωcm . The amounts of dopant added to the melt prior to the growth of these ingots are shown in Table I. Note that the actual dopant concentrations in the wafers will be affected by segregation during ingot growth, and will vary from the initial melt concentration.

High-purity feedstock and dopant sources were used during ingot growth, hence we do not expect significant quantities of unintended dopants. The interstitial oxygen concentrations were measured by room temperature Fourier-Transform Infrared Spectroscopy (FTIR) [5], and were between 18 and 23 ppm. Hence there is likely to be lifetime degradation in these wafers after exposure to significant amounts of illumination due to the boron-oxygen defect. The wafers were initially only 150-160 μm thick, and had a random pyramid texture on both surfaces. In order to achieve a planar surface for optimum surface passivation, the samples were polish-etched, resulting in final thicknesses of 65 to 130 microns.

After etching and cleaning, some wafers were subject to a 700°C, 35 minute anneal in nitrogen gas to remove any thermal donors [6,7], although we subsequently found there was no detectable difference between these wafers and the corresponding non-annealed samples, either in terms of resistivity or carrier lifetimes. After further cleaning, all samples were coated at 400°C with plasma-enhanced chemical vapour-deposited silicon nitride for surface passivation, followed by a 400°C forming gas anneal for 20 minutes, which we have found improves the surface passivation. Effective carrier lifetimes were then measured with the QSSPC technique [8].

Due to the thinness of the samples, it should be acknowledged that the effective lifetimes may contain a significant component due to surface recombination,

Table I. Parameters for the wafers from the five different ingots studied.

Ingot	Compensated?	Boron added to melt (cm ⁻³)	Phos. added to melt (cm ⁻³)	Measured resistivity (Ωcm)	Final wafer thickness (μm)
#74	No	0.35 × 10 ¹⁶	nil	4.4	70-100
#72	No	1.75 × 10 ¹⁶	nil	1.0	65-90
#73	No	5.0 × 10 ¹⁶	nil	0.40	100-130
#45	Yes	3.25 × 10 ¹⁶	2.75 × 10 ¹⁶	1.6	65-75
#44	Yes	7.5 × 10 ¹⁶	5.0 × 10 ¹⁶	0.47	90-130

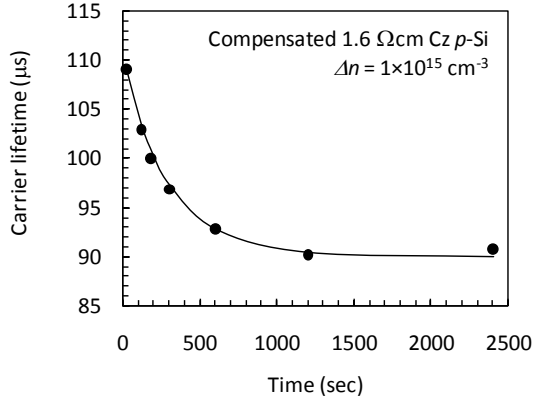


Figure 1. Reduction in lifetime as a function of time for a 1.6 Ωcm compensated wafer as FeB pairs re-form after dissociation by illumination. The lifetime was measured at an excess carrier density of $1 \times 10^{15} \text{ cm}^{-3}$. The solid line shows an exponential fit with a time constant $\tau_{\text{assoc}} = 330 \text{ s}$.

despite the presence of the passivating films. In principle, this could cause spurious differences between the compensated and non-compensated samples of similar resistivity. Table I lists the average thickness, among other parameters, for the wafers from each of the ingots studied. It shows that the thicknesses of the 1.0 Ωcm (control) and 1.6 Ωcm (compensated) wafers are similar, as are the 0.40 Ωcm (control) and 0.47 Ωcm (compensated) wafers. Therefore, any impact of the surface recombination should not greatly affect a comparison of carrier lifetimes between these two sets of wafers. Other aspects of the impact of surface recombination on the measured lifetimes are discussed in more detail below.

3 MEASURING DOPANT CONCENTRATIONS IN COMPENSATED SILICON

The concentrations of dopants in compensated material are sometimes determined via low-temperature photoluminescence (PL) [9,10] or infrared absorption (IR) measurements [11,12]. Both methods require low temperatures (between 4.2 and 15 Kelvin) and are mostly used for dopant concentrations below 10^{16} cm^{-3} , for which they are well characterized, but which is perhaps too low for some compensated solar-grade silicon. Higher dopant concentrations may be measured by physical techniques such as Secondary Ion Mass Spectrometry (SIMS) or Glow-Discharge Mass Spectrometry (GDMS). However, these techniques measure total concentrations, not only the electrically-active component, and are not commonly available in

photovoltaic laboratories (as is also true for low temperature PL and IR).

In this study we present an alternative method for determining the concentration of electrically-active acceptors in compensated *p*-type silicon, based on carrier lifetime measurements of the formation rate of iron-acceptor pairs at room temperature. The concentration of electrically-active donors can then also be inferred. The technique is described in more detail elsewhere [13], but we give an outline of it here, and describe its application to the samples in this study.

The wafers used in this work were found to contain trace amounts of interstitial iron, which can be detected by measuring the carrier lifetime before and after illuminating the sample with strong white light. This light breaks any Fe-acceptor pairs that form naturally at room temperature in *p*-type silicon, causing a change in lifetime that can be used to determine the interstitial iron concentration [14,15]. The Fe-acceptor pairs then slowly re-form as the interstitial iron diffuses to an acceptor atom and is trapped there by the coulombic attraction caused by their opposite charge. This process is limited by the diffusion of Fe at room temperature, which is well known, and the concentration of acceptor atoms in the sample. Hence, the rate at which the lifetime relaxes back to its initial value is related directly to the concentration of ionised acceptors in the wafer. The time constant for the relaxation of the lifetime (or pair association) is known as τ_{assoc} , and is related to the acceptor concentration via [16]:

$$\tau_{\text{assoc}} = 5.0 \times 10^5 \frac{T}{N_A} \exp(0.66/kT),$$

where the temperature T is measured in Kelvin ($T = 304 \text{ K}$ in this work), and τ_{assoc} is in seconds.

A typical lifetime decay after FeB pair dissociation is shown in Figure 1, for a wafer from the 1.6 Ωcm compensated ingot #45, measured at an excess carrier density of $\Delta n = 1 \times 10^{15} \text{ cm}^{-3}$. This data can easily be re-plotted as the dimensionless interstitial iron concentration $[\text{Fe}_i] = 1/\tau_{\text{initial}} - 1/\tau_{\text{final}}$, where τ_{final} is the lifetime after the decay is complete [16]. When plotted on a log-scale the exponential nature of this decay is evident, and the time constant τ_{assoc} can be extracted from a linear fit. These are shown in Figure 2 for wafers from the compensated ingots #44 and #45, and the control ingots #72 and #73.

Table II lists the values of τ_{assoc} determined in this way, and the corresponding N_A values for each of the ingots studied. Also shown for the non-compensated ingots are the N_A values calculated from the measured resistivities ρ via $1/\rho = q\mu_h p_0$, where q is the electronic charge, μ_h the majority hole mobility, and p_0 the

Table II. Measured parameters for the five ingots studied: measured resistivities and the corresponding boron concentrations N_A for the non-compensated control ingots, measured iron-acceptor re-pairing time constants τ_{assoc} , the corresponding boron concentrations N_A , the estimated donor concentrations N_D , the hole mobilities determined using Reggiani's model, and the N_A and N_D values determined by GDMS.

Ingot	Measured resistivity ρ (Ωcm)	N_A from resistivity (cm^{-3})	τ_{assoc} (s)	N_A from τ_{assoc} (cm^{-3})	Estimated N_D (cm^{-3})	μ_h (cm^2/Vs) (Reggiani's model)	N_A from GDMS	N_D from GDMS
#74	4.4	0.32×10^{16}	3700	0.36×10^{16}	nil	440	$< 10^{16}$	$< 10^{15}$
#72	1.0	1.5×10^{16}	800	1.7×10^{16}	nil	410	1.4×10^{16}	$< 10^{15}$
#73	0.40	4.3×10^{16}	310	4.3×10^{16}	nil	367	5.0×10^{16}	$< 10^{15}$
#45	1.6	–	330	4.0×10^{16}	2.9×10^{16}	362	4.3×10^{16}	3.0×10^{16}
#44	0.47	–	165	8.1×10^{16}	4.0×10^{16}	323	8.2×10^{16}	4.1×10^{16}

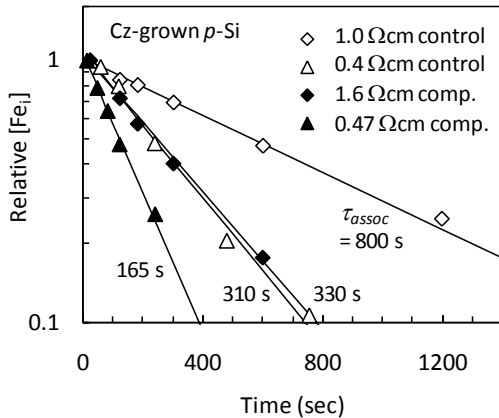


Figure 2. Exponential decays of the relative interstitial iron concentration for several compensated and non-compensated samples. The solid lines show exponential fits, with the time constants τ_{assoc} also shown.

equilibrium hole concentration. For the non-compensated ingots, $p_0 = N_A$. The mobilities were determined self-consistently using the model of Reggiani [17]. Note that for the three non-compensated control ingots, the N_A values determined via iron-acceptor pairing are in good agreement with the values determined via the measured resistivities. This indicates that the iron-acceptor pairing approach is an accurate way to determine N_A , and that the majority carrier mobilities in these wafers are close to the values predicted by the empirical model of Reggiani.

Taking the values for N_A as determined by iron-acceptor pairing in the compensated ingots, we may then also estimate the ionized donor concentration N_D in these samples. Assuming that $p_0 = N_A - N_D$, and again using Reggiani's mobility model [17] to estimate the hole mobility in the presence of both n - and p -type dopants, we can adjust N_D and the corresponding μ_h until the resulting resistivity $1/\rho = q\mu_h p_0$ is in agreement with the measured value. The values of N_D determined in this way are also shown in Table II.

In order to verify the accuracy of this technique, samples from each ingot were analysed using Glow-Discharge Mass Spectrometry (GDMS) at SINTEF [18]. The samples were pre-sputtered for about 5 minutes to remove surface contamination, with a sputtering rate of approximately 20 nm/s. The Relative Sensitivity Factors (RSFs) for this apparatus were found to be between 1.5 and 2 for boron, and 1 for phosphorus. Here we have assumed an RSF of 1.75 for determining the boron concentration. The results of the GDMS analysis are

shown in Table II. They are in good agreement with the boron and phosphorus concentrations obtained via the iron-acceptor pairing method, indicating that the latter technique is reliable.

This method for determining N_A and then N_D in compensated silicon seems to work reliably even when the iron concentration is very small, i.e. when the change in lifetime after illumination is also very small. In fact the lifetime in the sample from ingot #44 (compensated, 0.47 Ωcm), only changed by 2% after breaking the FeB pairs. Also note that this method for determining N_A is not affected by variations in the carrier mobility that can be caused by compensation, since the re-pairing rate measured is determined by the movement of Fe_i , not carriers. On the other hand, estimating N_D via the resistivity, as described above, does require knowledge of the hole mobility. If there is insufficient Fe in a sample to allow the method to be used, Fe could potentially be added deliberately in sacrificial test wafers, by implantation of Fe and annealing, or by annealing in a 'dirty' environment. Note, however, that we have found suitable traces of iron in almost all Cz-grown p -type wafers we have measured, and also in many float-zone wafers. Multicrystalline silicon wafers grown for solar cells always contain sufficient interstitial iron for these purposes, at least in the as-cut state, courtesy of contamination from the crucible [19,20].

Finally, the method is valid for any acceptor species, for example B, Ga or Al, or indeed a mixture of more than one species, since the re-pairing rate is independent of acceptor species [16]. The technique is more sensitive than other methods such as SIMS or GDMS for determining dopant concentrations in compensated material. It can also be performed relatively easily with standard lifetime measuring equipment.

4 EFFECTIVE LIFETIMES IN COMPENSATED SILICON

Figure 3 shows the effective lifetimes measured on the compensated and non-compensated wafers as a function of resistivity. There appears to be a measurable reduction in the lifetime of the compensated samples, by approximately a factor of two. Note that the lifetimes have been measured at an excess carrier density of $\Delta n = 1 \times 10^{15} \text{cm}^{-3}$ after a brief (1 minute) light-soaking to dissociate the FeB pairs. This gives the highest lifetime value, and hence the best comparison between samples when attempting to distinguish any lifetime reduction due

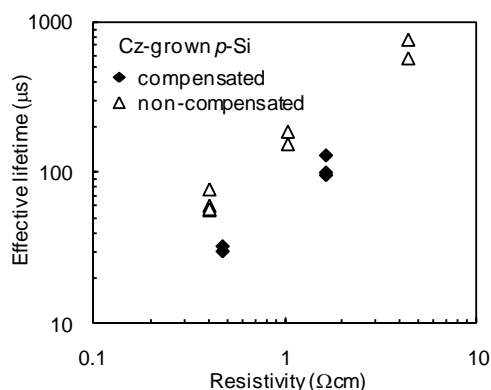


Figure 3. Effective lifetimes measured on compensated and non-compensated silicon wafers, as a function of resistivity. Prior to light-induced degradation.

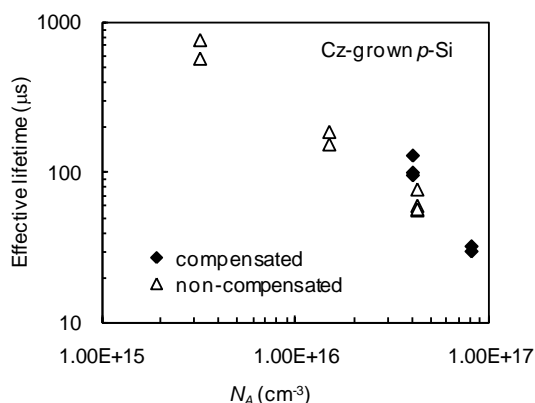


Figure 5. Effective lifetimes measured on compensated and non-compensated silicon wafers, as a function of the acceptor concentration N_A . Prior to light-induced degradation.

to compensation effects.

However, it may be misleading to compare these samples on the basis of resistivity, since the reduced mobilities in compensated material will cause a reduced resistivity for samples of the same net doping. A more appropriate parameter for comparison is the equilibrium majority carrier concentration p_0 , which is equal to the net doping $N_A - N_D$. It is this parameter which determines the recombination activity of defects and impurities at either the surfaces or in the bulk, and also the device voltage. The effective lifetime results are plotted again as a function of p_0 in Figure 4, with the $p_0 = N_A - N_D$ values based on the results of the iron-acceptor pairing method taken from Table II. Despite this slight adjustment, the apparent reduction in effective lifetime for the compensated samples remains.

There are several possible explanations for this reduced lifetime, which will be discussed in turn below. Note, however, that surface recombination is not likely to be the cause. It is often observed experimentally that the surface recombination velocity in low- or mid-injection increases approximately linearly with p_0 , as can be explained by Shockley-Read-Hall theory [21]. The dashed line in Figure 4 represents such a surface limitation on the effective lifetime, showing the most extreme surface-limiting conditions in which the control samples are assumed to be almost entirely surface-

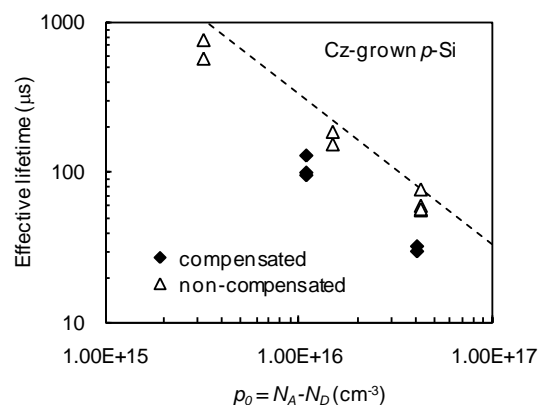


Figure 4. Effective lifetimes measured on compensated and non-compensated silicon wafers, as a function of the equilibrium majority hole concentration p_0 . Prior to light-induced degradation. The dashed line represents a possible surface-limited lifetime.

limited. It is clear that the compensated samples fall below this line, indicating an additional bulk recombination component in comparison with the control samples. It is true that the surface limit on the effective lifetime depends upon the wafer thickness, and that the thickness of these wafers varies considerably. However, as mentioned above, the control and compensated samples of similar p_0 values have comparable thicknesses. It therefore seems unlikely that surface recombination can explain the reduction in effective lifetime observed in the compensated wafers.

Figure 5 shows this data gain, but this time plotted as a function of the acceptor (boron) concentration N_A only. Although our data set is not large enough to rule out the possibility of a coincidence, this plot could imply that the extra recombination seen in the compensated material may be related to the additional boron.

This leads us to one possible explanation for the observed reduction in lifetime. It may be that the additional dopant atoms in the compensated material create recombination-active complexes. A well-known example is the boron-oxygen defect, which is activated by illumination [1]. It may also be that other dopant-related complexes are present. Note, however, that the data shown in Figures 3, 4 and 5 were measured without exposure to significant amounts of illumination, and that the samples had previously received a forming gas anneal at 400°C. Therefore the B-O defect should not have been activated. However, it is possible that this defect may slightly impact the lifetime even in the passive state, or that it was partially activated during the short light-soaking to dissociate FeB pairs. This could, in principle, explain the additional reduction in the compensated material.

To study this aspect in more detail, a different set of passivated samples were exposed to a long illumination to activate the B-O defect. As expected, the lifetimes degraded significantly. If recombination in the samples is then dominated by this defect, the lifetime measured at an excess carrier density equal to 10% of the net background doping can be estimated according to the expression of Bothe *et al.* [22]. This data is shown in Figure 6 for both the compensated and non-compensated material, plotted as a function of the boron concentration N_A . The dashed line represents Bothe's limit, and decreases

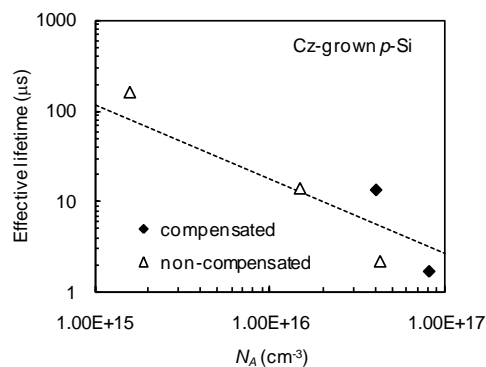


Figure 6. Effective lifetimes measured on compensated and non-compensated silicon wafers, as a function of the acceptor concentration N_A , after light-induced degradation. The dashed line represents the expected lifetime due to the B-O defect according to Bothe *et al.*

approximately linearly with N_A , since the defect is thought to contain a single boron atom. Surprisingly, the result for the less heavily-doped compensated wafer lies well *above* this limit. Re-plotting the data as a function of p_0 instead of N_A , as shown in Figure 7, results in a better agreement between the controls and the compensated wafers, and with Bothe's result. It is difficult to explain this observation, since in principle the concentration of B-O defects should scale with the B concentration N_A . More data is required to conclusively confirm or disprove the expected correlation between the degraded lifetime in compensated silicon and N_A .

A further potential explanation for the lifetime reduction in the compensated material, prior to activation of the B-O defect, is that unwanted contaminants may have been accidentally added to the melt along with the additional dopants. We can perform a crude check on this possibility by measuring the concentration of interstitial iron $[Fe_i]$ contamination in these wafers [14,15], assuming that iron is one of the contaminants accidentally added in this way. We must also assume that the wafers come from similar parts of the ingots in order to yield similar degrees of segregation of iron during crystallisation. To determine $[Fe_i]$ we have measured the lifetime before and after FeB pair breaking, and calculated the $[Fe_i]$ using a conversion factor C determined with p_0 and energy levels and capture cross section values from the literature [23]. Figure 8 shows the $[Fe_i]$ as a function of the total dopant concentration (i.e. both boron and phosphorus) added to the melt, taken from Table I. Although not conclusive, there does not appear to be a clear trend, suggesting that the iron may not come from the dopant sources. However, this does not rule out the possibility of other lifetime-limiting impurities being introduced along with the dopants.

Another possible explanation is that the compensated minority-dopant phosphorus atoms themselves act as mild recombination centres, based on their potential to attract minority carriers, as has been postulated recently [2]. Indeed, in this study we observe that the additional recombination is greatest for the compensated ingot with the most phosphorus added. However, this is far from proof of such an effect, and our results do not allow a more definite conclusion on this possibility. If it were shown to be true, it would represent an unavoidable additional source of recombination in compensated

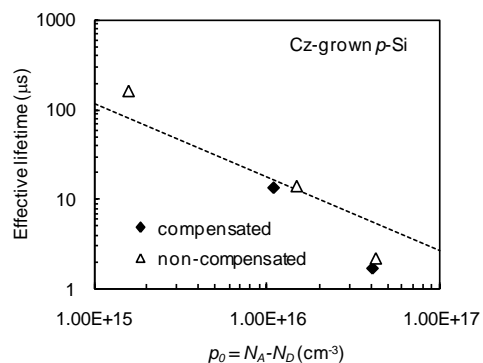


Figure 7. Effective lifetimes measured on compensated and non-compensated silicon wafers, as a function of the net doping p_0 , after light-induced degradation. The dashed line represents the expected lifetime due to the B-O defect according to Bothe *et al.*, but with p_0 substituted for N_A .

silicon. Similar studies on, for example, float-zone silicon (with low oxygen content), or n -type Cz, would allow the impact of the B-O defect to be more easily isolated. This would allow the possible role of the minority dopant atoms themselves in recombination to be assessed more directly.

Finally, it should be noted that reduced mobilities in strongly compensated material would have an impact on lifetimes measured by the QSSPC technique, as discussed below. A quantitative assessment of this effect would require independent measurements of the majority and minority carrier mobilities in compensated silicon, a task which is currently in progress. However, at this stage it seems unlikely that reduced mobilities can account for the large differences in lifetimes observed here between the compensated and non-compensated material of similar net doping.

To summarise these points, there is some evidence for a reduction in the bulk lifetime in compensated p -type Cz silicon when comparing samples with similar net doping levels. However, the data does not allow us to clearly identify the source of this additional bulk recombination – it may be due to dopant-related recombination complexes (for example the B-O defect, or others), or recombination activity of the minority-dopant atoms themselves, or indeed unintended contamination in the dopant material added to the melt (although this seems unlikely). In any case, coupled with the expected reduction in mobility in compensated material, there is reason for caution in using such material for solar cells. In some 'dirty' materials the presence of other impurities or defects reduces the lifetime further and may dominate recombination, in which case the effect of the reduction due to compensation alone may not be important.

5 CARRIER MOBILITIES IN COMPENSATED SILICON

In this section we present some preliminary, indirect evidence of reduced mobilities in the compensated wafers. Note that this is expected according to Reggiani's model [17], which predicts a reduction in mobilities in compensated material compared to non-compensated

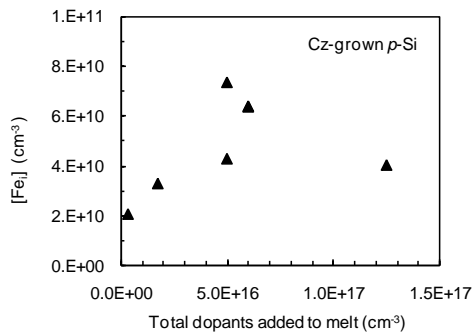


Figure 8. Interstitial iron concentration as a function of the total dopant concentration added to the melt.

silicon of the same net doping. This is caused by additional scattering from the extra charged dopant atoms, and although Reggiani's model was not developed specifically for the case of compensated silicon, we may use it as a guide since it accounts for both majority and minority carrier scattering from charged dopant atoms.

Our evidence comes via a comparison of carrier lifetimes measured with different techniques. The first of these techniques is QSSPC, which is directly affected by the carrier mobilities (in fact it measures the conductance, which is proportional to the lifetime-mobility product). The other techniques are Modulated Free-Carrier Absorption (MFCA) and Microwave Photoconductance Decay (μ W-PCD), neither of which are directly sensitive to the mobilities, and do not require knowledge of them to calculate the lifetime from the measured signal. (Despite its name, μ W-PCD measures reflectance, which is directly related to the carrier concentration rather than the conductance, and is in any case a transient technique.) This approach is similar in principle to that proposed by Neuhaus, in which QSSPC and Suns- V_{OC} data are compared in order to extract the sum of the minority and majority carrier mobilities [24].

Wafers from ingots #45 and #72, the first of which is compensated, and which have similar resistivities and p_0 values, were subject to full degradation via illumination to activate the boron-oxygen defect. Their lifetimes as measured by μ W-PCD were within 20% of each other, as they were also for MFCA measurements with the same bias light intensity. However, the lifetime derived from QSSPC data at the same generation rate for sample #45 was reduced by a further 30-40% compared to sample #72. This may indicate a reduced mobility in the compensated sample.

As can be seen in Table II, Reggiani's mobility model predicts a mobility reduction for majority carriers of only about 12% for this compensated ingot compared to the non-compensated one. However, for minority carriers, the expected reduction is larger - 33%. Combining these, the reduction in the sum of the mobilities is 28%, which might explain the observed difference between the lifetime techniques. For an exact comparison with QSSPC, the differential lifetimes measured by MFCA or μ W-PCD should be integrated with increasing bias light intensity [25]. Such an analysis is in progress. Comparison of QSSPC data with independently calibrated photoluminescence lifetime data would also be interesting in this regard.

6 CONCLUSIONS

Compensation leads to some interesting effects in silicon wafers that could be important for device performance. We have found evidence for a reduction in the bulk lifetime of compensated wafers when compared to non-compensated wafers of similar net doping. At this stage we cannot clearly identify the source of this recombination, assuming it is not an artefact related to reduced mobilities. Despite this potential lifetime reduction, compensation may still be of net benefit when applied to material that would otherwise be of much too low resistivity to be used for cell production. We have also presented a technique for measuring the total acceptor and donor concentrations in compensated p -type silicon wafers.

Acknowledgments: The authors are grateful to Kai Petter of Q-cells for kindly supplying the wafers used in this study. We also thank Chris Samundsett and Eugenia Sepulveda for assistance with sample preparation, and Jessica De Wild and Gianluca Coletti for the lifetime data on degraded wafers. This work has been supported by the Australian Research Council and SenterNovem, The Netherlands.

- [1] J. Schmidt and K. Bothe, *Physical Review B* 69 (2004) 024107.
- [2] L. J. Geerligs, D. Macdonald and G. Coletti, 17th NREL Workshop on Crystalline Silicon Solar Cells & Modules: Materials and Processes, Vail, Colorado (2007)
- [3] S. Dubios, N. Enjalbert and J. P. Garetet, *Applied Physics Letters* 93 (2008) 032114.
- [4] L. J. Geerligs and D. Macdonald, *Progress in Photovoltaics: Research and Applications* 12 (2004) 309.
- [5] A. Baghdadi, *et al.*, *Journal of the Electrochemical Society* 136 (1989) 2015.
- [6] C. Hässler, *et al.*, *Materials Science and Engineering B* 71 (2000) 39.
- [7] P. Wagner and J. Hage, *Applied Physics A: Solids and Surfaces* 49 (1989) 123.
- [8] R. A. Sinton and A. Cuevas, *Applied Physics Letters* 69 (1996) 2510.
- [9] P. M. Colley and E. C. Lightowers, *Semiconductor Science and Technology* 2 (1987) 157.
- [10] G. Davies, *Physics Reports* 176 (1989) 83.
- [11] B. O. Kolbesen, *Applied Physics Letters* 27 (1975) 353.
- [12] S. C. Baber, *Thin Solid Films* 72 (1980) 201.
- [13] D. Macdonald, A. Cuevas and L. J. Geerligs, *Applied Physics Letters* 92 (2008) 202119.
- [14] G. Zoth and W. Bergholz, *Journal of Applied Physics* 67 (1990) 6764.
- [15] D. Macdonald, L. J. Geerligs and A. Azzizi, *Journal of Applied Physics* 95 (2004) 1021.
- [16] D. Macdonald, T. Roth, P. Deenapanray, K. Bothe, P. Pohl and J. Schmidt, *Journal of Applied Physics* 98 (2005) 083509.
- [17] S. Reggiani, *et al.*, *IEEE Transactions on Electron Devices* 49 (2002) 490.

- [18] M. DiSabatino, A. L. Dons, J. Hinrichs, O. Lohne and L. Arnberg, Proceedings 22nd European Photovoltaic Solar Energy Conference, Milan, Italy (2007) 271.
- [19] T. Buonassisi, *et al.*, Progress in Photovoltaics: Research and Applications 14 (2006) 513.
- [20] E. Olsen and E. J. Øvrelid, Progress in Photovoltaics: Research and Applications 16 (2008) 93.
- [21] A. G. Aberle, "*Crystalline Silicon Solar Cells: Advanced Surface Passivation and Analysis*", University of New South Wales, Sydney, 1999.
- [22] K. Bothe, R. Sinton and J. Schmidt, Progress in Photovoltaics: Research and Applications 13 (2005) 287.
- [23] D. Macdonald, T. Roth, P. N. K. Deenapanray, T. Trupke and R. A. Bardos, Applied Physics Letters 89 (2006) 142107.
- [24] D. H. Neuhaus, P. P. Altermatt, A. B. Sproul and A. G. Aberle, Proceedings 17th European Photovoltaic Solar Energy Conference, Munich, Germany (2001) 242.
- [25] A. G. Aberle, J. Schmidt and R. Brendel, Journal of Applied Physics 79 (1996) 1491.